This is a repository copy of *Characterizing cross-linking within polymeric biomaterials in the SEM by secondary electron hyperspectral imaging*.

White Rose Research Online URL for this paper:
https://eprints.whiterose.ac.uk/154872/

Version: Published Version

Characterizing Cross-Linking Within Polymeric Biomaterials in the SEM by Secondary Electron Hyperspectral Imaging

Nicholas Farr,* Samand Pashneh-Tala, Nicola Stehling, Frederik Claeyssens, Nicola Green, and Cornelia Rodenburg

A novel capability built upon secondary electron (SE) spectroscopy provides an enhanced cross-linking characterization toolset for polymeric biomaterials, with cross-linking density and variation captured at a multiscale level. The potential of SE spectroscopy for material characterization has been investigated since 1947. The absence of suitable instrumentation and signal processing proved insurmountable barriers to applying SE spectroscopy to biomaterials, and consequently, capturing SE spectra containing cross-linking information is a new concept. To date, cross-linking extent is inferred from analytical techniques such as nuclear magnetic resonance (NMR), differential scanning calorimetry, and Raman spectroscopy (RS). NMR provides extremely localized information on the atomic scale and molecular scale, while RS information volume is on the microscale. Other methods for the indirect study of cross-linking are bulk mechanical averaging methods, such as tensile and compression modulus testing. However, these established averaging methods for the estimation of polymer cross-linking density are incomplete because they fail to provide information of spatial distributions within the biomaterial morphology across all relevant length scales. The efficacy of the SE spectroscopy capability is demonstrated in this paper by the analysis of poly(glycerol sebacate)-methacrylate (PGS-M) at different degrees of methacrylation delivering new insights into PGS-M morphology.

The potential of secondary electron (SE) spectroscopy for material characterization has been investigated as far back as 1947.[1] However, it is only with recent advancements in instrumentation,

N. Farr, Dr. S. Pashneh-Tala, Dr. N. Stehling, Dr. F. Claeyssens,
Dr. N. Green, Dr. C. Rodenburg
Department of Materials Science and Engineering
Sir Robert Hadfield Building
Mappin Street, Sheffield S1 3JD, UK
E-mail: nfarr1@sheffield.ac.uk
Dr. N. Green
INSIGNEO Institute for In Silico Medicine
The Pam Liversidge Building
Sir Robert Hadfield Building
Mappin Street, Sheffield S1 3JD, UK

signal processing, and imaging capability that SE spectroscopy can be exploited to open up a new realm of opportunities for novel material characterization of polymers in the scanning electron microscope (SEM) by SE hyperspectral imaging (SEHI). While in a standard SEM an image is formed from all detected SEs that are emitted from a surface regardless of their energy, in SEHI a series of images is collected, each of which is created using SEs from a defined energy band. Such SEHI image series can then be used to extract a SE spectrum. In the last 5 years, SEHI has been deployed in a wide variety of applications, but in particular, for the mapping of semi-crystalline polymers, exploring the molecular orientation of organic electronic devices, and recently revealing nanostructure variations within natural materials.[2,3] Here we show that the SEHI approach can be also utilized as a novel characterization tool to map cross-link densities in beam sensitive biomaterials.

Polymer cross-links are the covalent bonds which are irreversibly formed between molecular chains of the polymer. Increasing the density of cross-links decreases the ability of polymer chains to slide over each other and accordingly increases the relative mechanical tensile strength of the polymer and its brittle fracture resilience.[4]

Therefore, a polymer-based biomaterial's cross-linking density is a major contributor to its mechanical properties.[5] For a polymer to be considered as a viable biomaterial, promotion of cell growth is essential. The ability of the biomaterial to promote cell growth is highly influenced by local surface variations that arise as a consequence of these mechanical properties. Localized variations in cross-linking density are important for the biocompatibility of the material and as yet there is no imaging tool available to assess such variations. This might seem surprising as it has been shown that cross-linking density is also associated with the biodegradation rate of biomaterial scaffolds and can be utilized as an effective control of biodegradation.[6]

Additionally, cross-linking has demonstrated an ability to suppress the immunogenicity of an implanted scaffold.[7] Thus the ability to quantify the extent and density of cross-linking is considered to be a key capability to promote the efficient development of effective biomaterials. The behavior and kinetics of the

**ADVANCED
SCIENCE NEWS**
www.advancedsciencenews.com

**Macromolecular
Rapid Communications**
www.mrc-journal.de

cross-linking processes of polymer-derived biomaterials have been previously surveyed by applying diverse analytical techniques such as nuclear magnetic resonance (NMR), differential scanning calorimetry, and Raman spectroscopy (RS). While NMR can provide extremely localized information on both the atomic scale and molecular scale, the RS information volume is typically on the microscale. Other available methods for the indirect study of the cross-linking structures of soft polymers are bulk mechanical averaging methods, such as tensile and compression modulus testing. However, these established averaging methods for the estimation of polymer cross-linking density are incomplete as they fail to provide information on spatial distributions within the biomaterial morphology across all relevant length scales.

To develop a comprehensive understanding of the key relationships between the biocompatibility of different polymer structures, the capability to reveal both nano- and microscale levels of structural detail is essential. Here we demonstrate that SEHI can provide structural detail information using poly(glycerol sebacate)-methacrylate (PGS-M) as an example.

PGS-M is an elastomeric degradable polymer and a functionalized form of the well-studied poly(glycerol sebacate) (PGS). PGS being a non-toxic tuneable polymer,[8,9] has become an interesting potential biomaterial in various promising applications such as supporting the growth of cardiac tissue,[10] blood vessels,[11,12] and cartilage.[13,14] PGS-M differs from PGS as a result of functionalization with methacrylate groups which causes the polymer to be photocurable. The photocurable capability of PGS-M enhances the existing strengths of PGS by allowing the material to be cross-linked at lower temperatures and pressures. This enables the precise fabrication of highly detailed microscale structures and the potential direct incorporation of cells or temperature sensitive molecules.[15] The ease with which PGS-M can be synthesized together with the adaptability of its physical properties and suitability for use with different cell types, makes PGS-M an attractive candidate for an extensively deployed biomaterial.[15] The adaptability relies on user-defined cross-linking as PGS-M can be photocured at various degrees of methacrylation and the degree of methacrylate (DM) used in its production has a direct relationship to the density of cross-linking. The greater the DM, the greater the average cross-linking density. Tensile testing has previously revealed that the mechanical properties of PGS-M varied in accordance with its morphology, both Young's modulus and UTS increased significantly with increasing levels of DM.[15,16] Further validation is required to confirm this relationship but PGS-M is generating much interest as a biomaterial. PGS-M is therefore considered an ideal model polymer to assess SEHI as a viable biomaterial cross-linking characterization technique.

In this study, SEHI will be applied to characterize the increasing cross-linking densities of PGS-M at three different DM levels: 30%, 50%, and 80%. Argon plasma treatment has been included in the study to initiate supplementary cross-linking variation within a single set of PGS-M samples.

Plasma modification of a polymeric biomaterial's surface layer is often carried out in order to: generate functional groups on its surface, change free surface energy, increase surface hydrophilicity or achieve hydrophobicity, change cross-linking of surfaces, change surface morphology, or remove impurities. Previous studies on PGS, which has a similar structure to PGS-M, have

observed that plasma treatment[17] intensified hydrophilicity, increased the capability of stimulating cell proliferation, and extracellular matrix production. Such studies have also indicated that plasma treatment has induced surface cross-linking within the chemically similar PGS, but as yet no technique has been able to map their existence[17] using traditional characterization methods, presumably due to a lack in surface sensitivity.

During plasma treatment inert gases are used to eliminate some of the atomic species from the polymer's surface, thereby producing reactive surface radicals. These radicals subsequently react within the surface structure forming chemical bonds, a process that has the potential to result in a cross-linked surface.[18] Argon plasma treatment is active in sputtering several nanometers of material from the sample surface, thus making surface modifications on a nanometer scale, which may be beneficial to the deployment of PGS-M as a biomaterial.[19] The purpose of the introduction of argon plasma treatment within the study will be to treat the surface of PGS-M and analyze the resulting cross-linking density on cross-sections of the material as a further illustration of lateral and depth mapping of cross-linking using SEHI.

Nanoindentation results displayed in **Figure 1**, showed a relationship between the increase in the degree of methacrylation and a subsequent increase in hardness and stiffness of the polymer. Alongside previous work this result corroborates the proposition that increasing the percentage of the degree of methacrylate (DM) used in the production of PGS-M has a direct relationship to the density of cross-linking observed.[15,16] The results also provide evidence that increasing DM does directly increase the hardness of the material and has a strong influence on its elastic modulus.

Figure 2A presents the results of Raman spectroscopy applied to the PGS-M samples with three different DM. The expected position of the first peak of interest is at 2200 cm^{-1} and relates to C=C bonding.[20] The weaker bonding energies of double bonds and acrylate groups are a common starting point for radical reactions like polymerization or cross-linking processes. Therefore, the absence of this peak in the observed results is a strong indication of the successful process of cross-linking and shows that polymerization is complete. The most prominent differences observed between PGS-M 30%, 50%, and 80% DM were in the spectral range around 2950 cm^{-1}. PGS-M photocured polymers show an increase of CH vibrations, specifically C—H alkyl, which is associated with the cross-linking of PGS-M after photo-polymerization. The asymmetric and symmetric stretching vibration of a methyl group usually occurs at about 2965 and 2880 cm^{-1}, respectively. Peaks in the data within this range consist of C–H vibrations with the intensity ratios having previously been related to composition and cross-linking.[21] Formation of the polymer network after successful photocuring of PGS-M can therefore be confirmed by identifying an increase in alkyl groups. This is a product of the elimination of acrylate groups,[22] which are observed through a corresponding increase in C–H vibrations. Furthermore, due to the small height of PGS-M samples, the observed signal included components detected at <1500 cm^{-1} which were generated by the underlying borosilicate glass. This is not an uncommon occurrence and has previously been documented to produce pronounced peaks in the fingerprint region.[15]
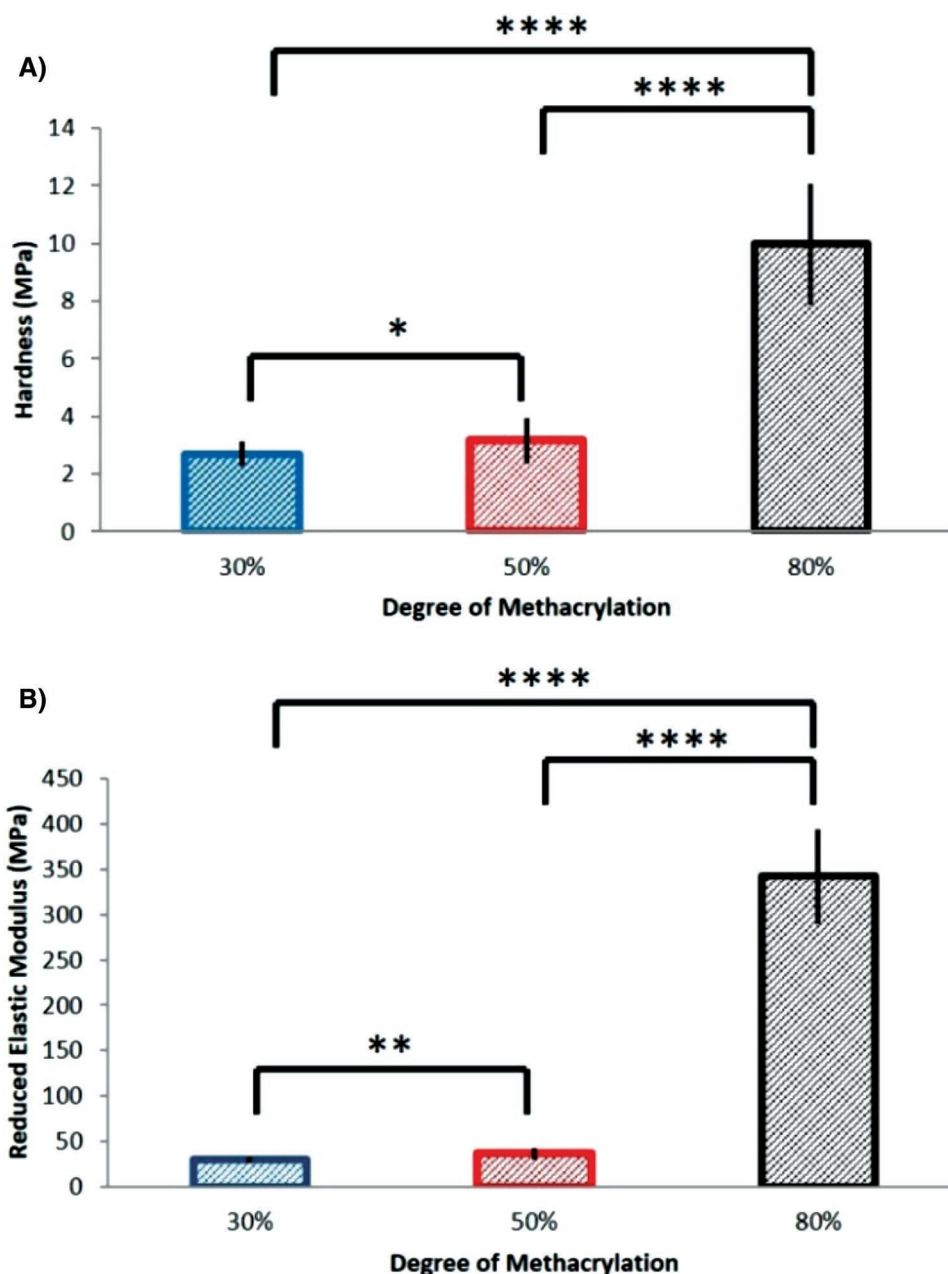
**ADVANCED
SCIENCE NEWS**
www.advancedsciencenews.com

**Macromolecular
Rapid Communications**
www.mrc-journal.de

Figure 1. A) Outlines the hardness (MPa) and B) reduced elastic modulus (MPa) obtained from nanoindentation for varying degrees of methacrylation of PGS-M (mean $\pm$ STD error bars). The degree of significance is indicated as ****$p < 0.0001$, ***$p < 0.001$, **$p < 0.01$, and *$p < 0.05$.

The SE spectra captured from the surfaces of PGS-M for the three specimens with different cross-linking densities are displayed in Figure 2B. It can be observed that the dominant peak intensity values rise as the DM-driven cross-linking density increases. This effect is prominent within the energy window of 2.9–4.3 eV for PGS-M. It has been recently established that SE emission 3.3–4.7 eV are attributable to hydrogenated carbon bonding. Abrams et al.[23] have shown by the results of an electron beam contamination study that amorphous contamination (hydrogenated carbon) deposits on carbon-based samples can be identified through energy peaks within the 3.3–4.7 eV range.

The peaks associated with hydrogenated carbon correlate with the observed C–H vibrations peak given in the captured Raman spectrum as predicted by these results. Figure 2C,D shows the change in the Raman data at 2950 cm^{-1} and SE emission change at 3.6 eV respectively, for PGS-M samples. The changes in Raman intensity at 2950 cm^{-1} (C–H vibrations) closely correlates with the SE intensity changes at 3.6 eV. Both peaks are similarly affected by CH bonding and consequently the cross-linking process of PGS-M. The correlation also holds for the relative integrated intensity for both Raman and SE emissions representing the wider to C–H vibrations windows
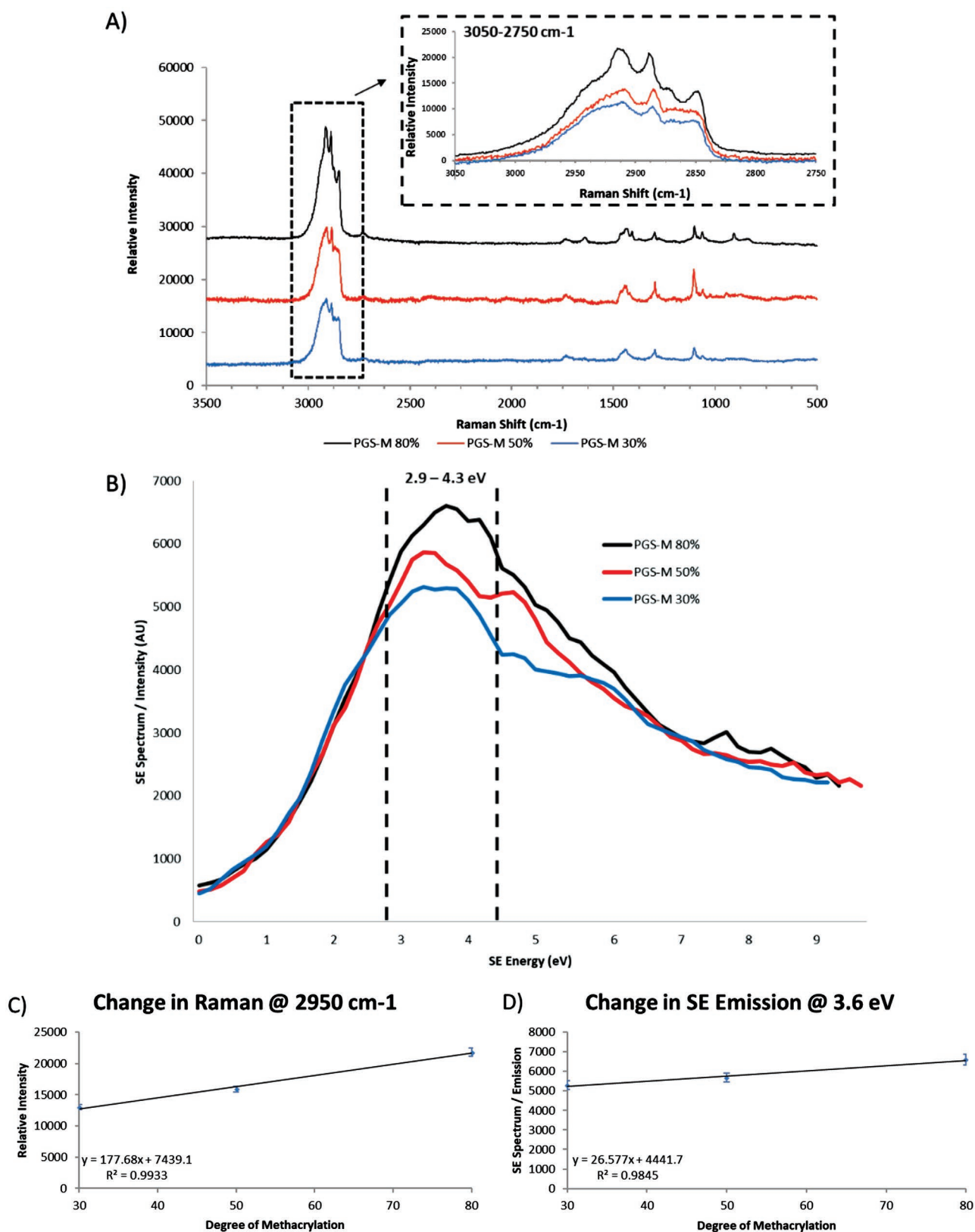
Figure 2. A) Offset Raman spectra for 30%, 50%, and 80% low-molecular-weight PGS-M. B) Secondary electron spectra for 30%, 50%, and 80% low-molecular-weight PGS-M. C) Raman peak values for 30%, 50%, and 80% low-molecular-weight PGS-M (*n* = 4) at 2950 cm^{-1} (mean ± STD error bars). D) Secondary emission values for 30%, 50%, and 80% low-molecular-weight PGS-M (*n* = 4) at 3.6 eV (mean ± STD error bars).

(Raman: 3000–2790 cm⁻¹ and SE energy region: 2.9–4.3 eV) as shown in Figure S4, Supporting Information. The consistency of SEHI results when compared to those of the Raman spectrum provides a strong argument that both the techniques possess the ability to detect cross-linking in PGS-M through CH bonding changes. However, SEHI displays the additional benefits of a multiscale imaging capability and thus the ability to capture spatial variations.

The SE spectrum also provides a new insight into a previously unknown link between DM and the heterogeneous/homogeneous structure of the PGS-M polymer. **Figure 3**A displays the standard deviation of the cross-linking variation between samples of PGS-M at 80% and 30% DM. The results reveal that PGS-M 30% DM displays a significantly greater variation than that of PGS-M at 80%. The evident increase in the variation in SE spectra values that represents cross-linking density across the polymer samples appears to correlate to a lower DM percentage. This is not unexpected as the chemical composition between samples will exhibit production variability. However, the variation detail observed in the SEHI data across the range of DM% provides an insight not available previously.

The ability of SEHI to isolate compositional chemical changes in both the micro- and nanoscale is expected to provide a novel capability for future work directed at analyzing cellular behavior within seeded biomaterials. As previously affirmed, other techniques that have been historically applied to quantifying cross-linking lack the ability for spatial mapping of the variation of the cross-linking within a sample across these length scales. This makes SEHI an especially useful technique to characterize cross-linking variations within a multiscale approach that provides the ability to map nanoscale variations in particular, if component analysis is used (see Figures S2, S3, and S5, Supporting Information).

In order to isolate cross-linking density as the major contributor to the peak intensity of SE emissions observed in the SEHI spectra, the potential contribution from PGS-M molecular weight was investigated. Comparison results of SEHI spectra of low- and high-molecular-weight forms of 30% PGS-M are displayed in Figure 3B. These results show that molecular weight has no direct impact on the relative intensity of the previously dominant (3.6 eV) peak. However, a new dominant peak around 2.1 eV was observed within the spectrum for the high-molecular-weight form (Figure 3B). Whilst all the spectra have broadly the same profile, some notable differences can be observed that are the consequence of variations in molecular ordering. Conspicuously, around 2.1 eV, the high-molecular-weight PGS-M sample is seen to display a clear peak whereas in the low-molecular-weight PGS-M sample a lesser peak is observable, resulting in only a slight change within the spectrum gradient around 2 eV. These differences can be attributed to the crystalline phases in the semi-crystalline PGS-M sample. This spectral association with increased molecular weight has not been previously observed. The region of these peaks are consistent with previously published work,[24] which show the shift to higher or lower energies is related to differences in the molecular order of the material. In this instance, the addition of a peak around 1.4–2.3 eV for high-molecular-weight PGS-M is considered a marker of a more crystalline state in high-molecular-weight when compared to that of low-molecular-weight PGS-M. The ability to observe and, ideally in a future capability, to quantify molecular weight ordering within polymer-derived biomaterials is considered to be an important development, particularly as molecular weight has been shown to have a strong influence on cellular growth.[25] Figure S2, Supporting Information, displays component analysis of captured SEHI image stacks that indicate 30% low-molecular-weight PGS-M possesses a measurably greater variation of lateral molecular weight composition than that observed for the 80% low-molecular-weight PGS-M sample. These variations are considered to be the consequence of different regions of the PGS-M samples containing dissimilar ratios of high-molecular-weight and low-molecular-weight structures as a result of an expected inconsistency in polymer curing. The approach of SEHI to construct spectra from a stack of images, captured from different deflector voltages, enables the option to further validate this hypothesis by examining each of the individual SEM images. The source SEM images shown in Figure 3B provide supporting evidence that a greater variation of structures is present on the high-molecular-weight PGS surface. It can therefore be seen that the elements of the SEHI approach are complementary and facilitate biomaterial characterization through multiple perspectives and has the ability to carry out depth analysis by using SEHI on cross-sections.

Figure 4A shows that there are variations in the PGS-M sample within the thickness of the sample. While there is only a slight intensity difference between surface and subsurface spectra in the region responding to cross-linking, the appearance of a dominant low energy peak around 2.2 eV within the subsurface PGS-M SE spectrum is indicative of variations in molecular weight. Some surface fragmentation, perhaps hydrolysis-driven surface degradation, would affect the ratio of crystalline and amorphous phases. The subsurface of PGS-M is assumed to be protected from such environmental factors and consequently exhibits a more ordered and crystalline structure. The observation of this low energy peak is consistent with previously documented changes in SE electron emission profiles in response to molecular ordering dissimilarities.[24] This proposed rationale for surface fragmentation is further supported by the slight reduction in cross-linking recorded in the intensity of the C−H bonding SE peak.

Figure 4B presents the SE spectrum of PGS-M after undergoing 100 W argon plasma surface treatment for 3 min. An SEM image of argon plasma treated cross-section of PGS-M distinctly shows morphology differences between an upper surface "crust" and the polymer's internal structure. Both surface and subsurface spectrums exhibit small molecular weight peaks at 2 and 1.6 eV respectively, slightly changing the gradient of each spectrum. However, in contrast to non-treated PGS-M samples, the 2.9–4.3 eV peaks associated with C–H vibrations are dominant. The fragmentation of molecular chains is expected to occur deeper than 50 µm.[26] This has resulted in the reduction of the molecular weight peak observable within the spectrum of subsurface argon plasma treated PGS-M in comparison to that of untreated subsurface PGS-M. The spectrum of the near surface of PGS-M collected post argon treatment indicates a clear increase in dominant
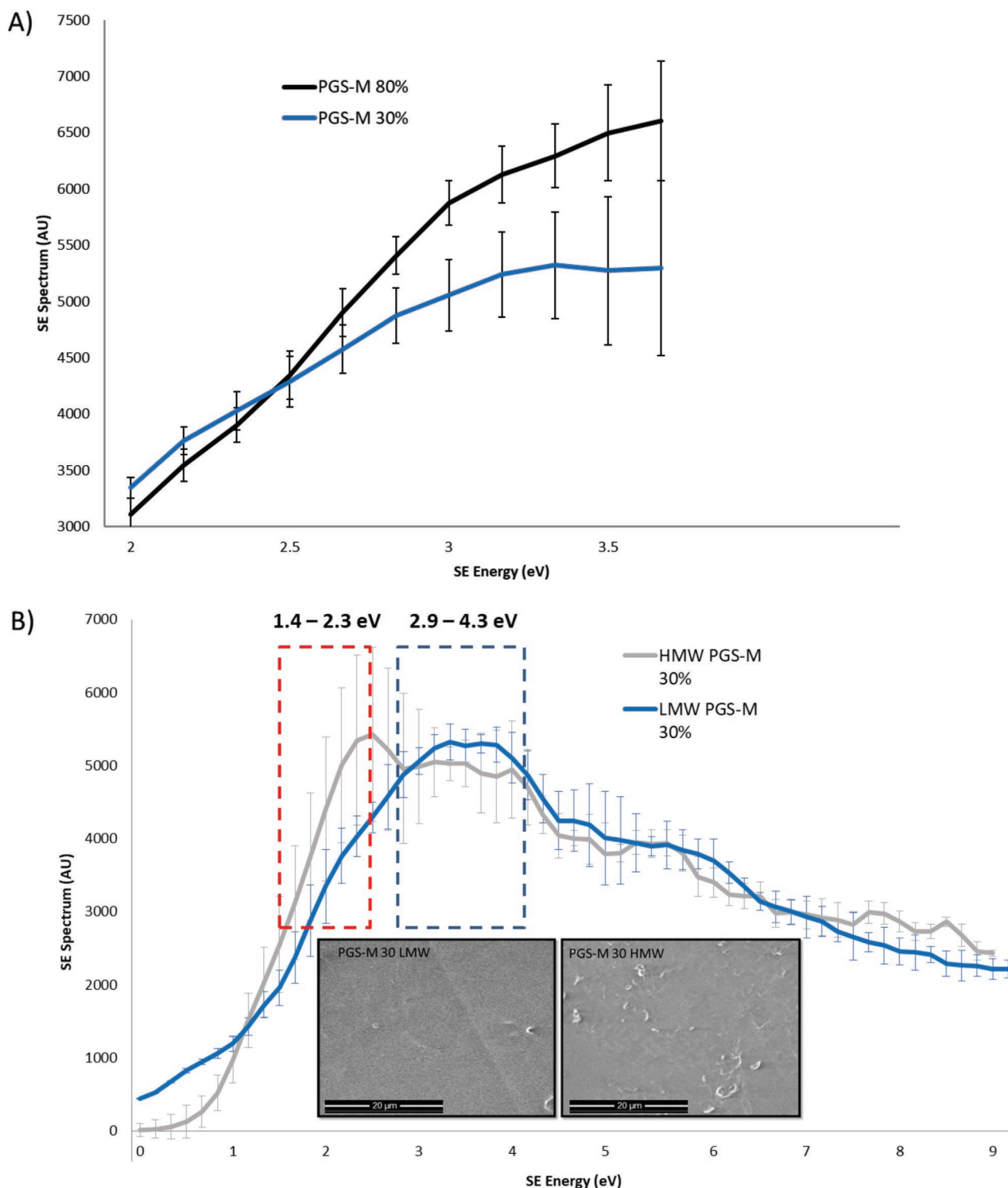
ADVANCED
SCIENCE NEWS
www.advancedsciencenews.com

Macromolecular
Rapid Communications
www.mrc-journal.de

Figure 3. A) Secondary electron spectra for 30% ($n = 4$) and 80% ($n = 4$) low-molecular-weight PGS-M isolating SD variation between 2–3.6 eV (mean $\pm$ STD error bars). B) Secondary electron spectra for 30% low- ($n = 4$) and high-molecular-weight ($n = 4$) (mean $\pm$ STD error bars). Inset SEM images show sub-micron variation visually between high- and low-molecular-weight PGS-M.

peak intensity compared to that of the subsurface spectrum. This indicates an increase of cross-linking within the surface of argon plasma treated PGS-M. It has long been established

that argon plasma has sufficient energy to produce radicals by breaking the C−H bonds. The recombination of these radicals leads to cross-linking of the molecular chains at the
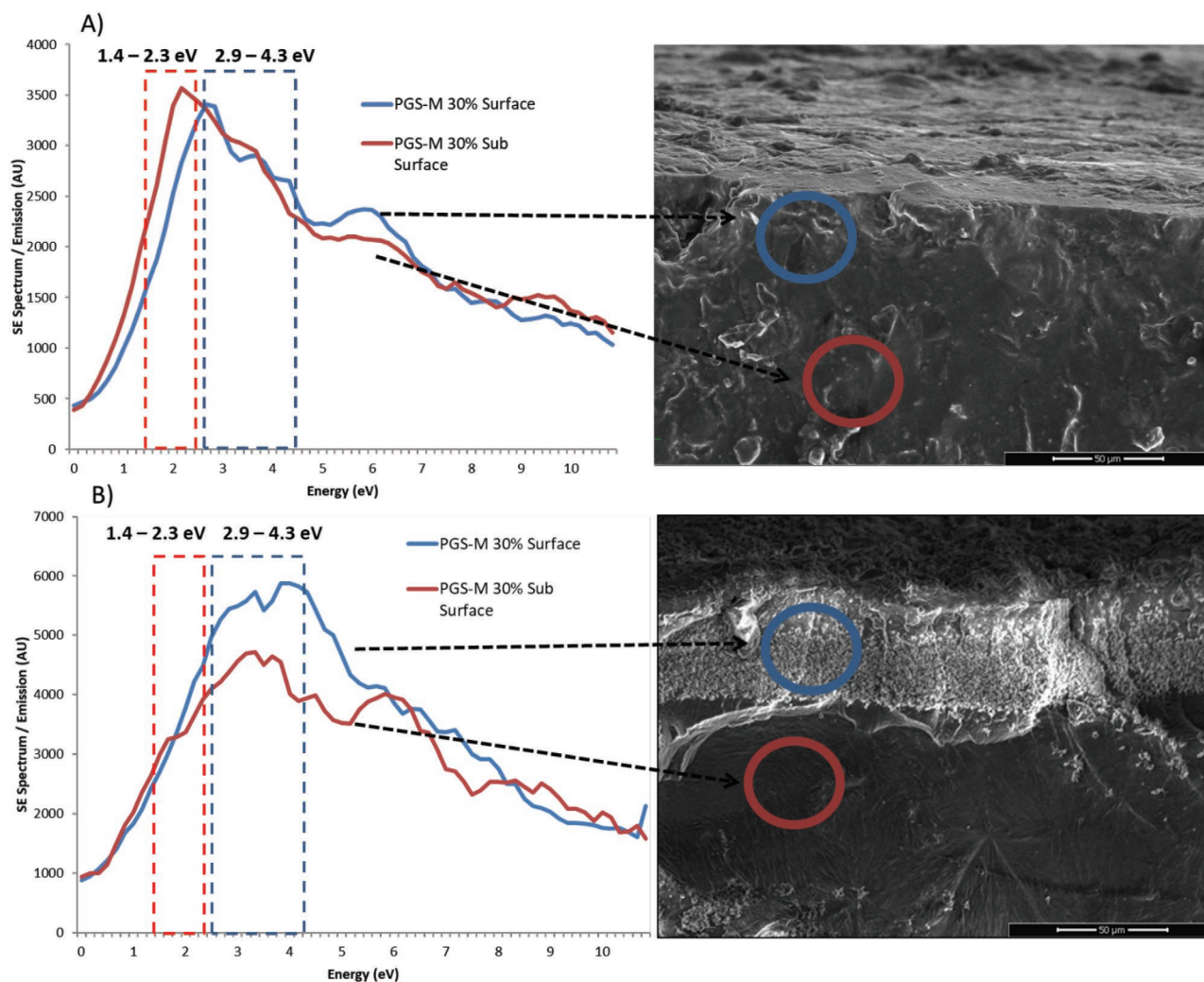
**ADVANCED
SCIENCE NEWS**
www.advancedsciencenews.com

**Macromolecular
Rapid Communications**
www.mrc-journal.de

Figure 4. A) Secondary electron spectra and SEM image for and of surface and subsurface 30% low-molecular-weight PGS-M. B) Secondary electron spectra and SEM image for and of surface and subsurface 30% low-molecular-weight argon plasma-treated PGS-M.

polymer surface. SEHI spectra displayed in Figure 4B has for the first time highlighted that post plasma treatment, there is an increase of cross-linking on the surface when compared to subsurface layers of PGS-M.

This future potential application of SEHI as a characterization tool for polymer-derived biomaterials is of interest as most polymer surfaces, especially hydrocarbon surfaces; are chemically inert, have low surface energies, and also exhibit low adhesion properties, all of which are disadvantageous for many biomaterial practical applications.

In conclusion, this study provides evidence that SEHI enables the mapping of cross-linking distribution at a multiscale level within a polymer (PGS-M). The SEHI capability to provide both nano- and microscale levels of detail of the morphology of biomaterials is considered to be a valuable tool, especially for polymer-based biomaterials. Here, cross-linking density and local variations in molecular order are major contributors to a biomaterial's mechanical properties and accordingly the consequential biocompatibility of the material. SEHI not only provides an alternative to contemporary analysis tools, but also provides researchers with a novel and enhanced nanostructure analysis capability for characterizing cross-linking and its spatial variation in beam sensitive biomaterials.

Supporting Information

Supporting Information is available from the Wiley Online Library or from the author.

Acknowledgements

Conflict of Interest

The authors declare no conflict of interest.

Keywords

[1] V. R. Kollafh, *Zur Energieverteilung der Sekundarelektronen I: Mepergebnisse und Diskussion. Annalen der Physik* **1947**, *1*, 357.

[2] Q. Wan, K. J. Abrams, R. C. Masters, A. C. S. Talari, I. U. Rehman, F. Claeyssens, C. Holland, C. Rodenburg, *Adv. Mater.* **2017**, *29*, 1703510.

[3] R. C. Masters, A. J. Pearson, T. S. Glen, F.-C. M. Sasam, L. Li, M. Dapor, A. M. Donald, D. G. Lidzey, C. Rodenburg, *Nat. Commun.* **2015**, *6*, 6928.

[4] A. W. Martinez, J. M. Caves, S. Ravi, W. Li, E. L. Chaikof, *Acta Biomater.* **2014**, *10*, 26.

[5] N. Reddy, R. Reddy, Q. Jiang, *Trends Biotechnol.* **2015**, *33*, 362.

[6] M. Bing, W. Xiaoya, W. Chengtie, C. Jiang, *Regener. Biomater.* **2014**, *1*, 81.

[7] Y. Wang, J. Bao, X. Wu, Q. Wu, Y. Li, Y. Zhou, L. Li, H. Bu, *Sci. Rep.* **2016**, *6*, 24779.

[8] Y. Wang, G. A. Ameer, B. J. Sheppard, R. Langer, *Nat. Biotechnol.* **2002**, *20*, 602.

[9] L. X. Jun, A. A. Karim, C. Owh, *J. Mater. Chem. B* **2015**, *3*, 7641.

[10] M. Kharaziha, M. Nikkhah, S.-R. Shin, N. Annabi, N. Masoumi, A. K. Gaharwar, G. Camci-Unal, A. Khademhosseini, *Biomaterials* **2013**, *34*, 6355.

[11] K. W. Lee, D. B. Stolz, Y. Wang, *Proc. Natl. Acad. Sci. USA* **2011**, *108*, 2705.

[12] W. Wu, R. A. Allen, Y. Wang, *Nat. Med.* **2012**, *18*, 1148.

[13] C. K. Hagandora, J. Gao, Y. Wang, A. J. Almarza, *Tissue Eng., Part A.* **2013**, *19*, 729.

[14] J. M. Kemppainen, S. J. Hollister, *J. Biomed. Mater. Res., Part A.* **2010**, *94A*, 9.

[15] S. Pashneh-Tala, R. Owen, H. Bahmaee, S. Rekštyte, M. Malinauskas, F. Claeyssens, *Front. Phys.* **2018**, *6*, 41.

[16] A. Singh, S. Asikainen, A. K. Teotia, P. A. Shiekh, E. Huotilainen, I. Qayoom, J. Partanen, J. Seppälä, J. V. Kumar, *ACS Appl. Mater. Interfaces.* **2018**, *8*, 11677.

[17] T. Theerathanagorn, J. Klangjorhor, M. Sakulsombat, P. Pothacharoen, D. Pruksakorn, P. Kongtawelert, W. Janvikul, *J. Biomater. Sci., Polym. Ed.* **2015**, *26*, 1386.

[18] S. Makoto, I. Taku, K. Masaru, N. Nobuyuki, T. Yasuhiko, Y. Hiroshi, *J. Micro/Nanolithogr., MEMS, MOEMS,* **2013**. *12*, 041309.

[19] Nordson MARCH, *AZoNano*, https://www.azonano.com/article.aspx?ArticleID=5207 (accessed: May 2019).

[20] R. M. Silverstein, G. C. Bassler, *J. Chem. Educ.* **1962**, *39*, 546.

[21] K. B. R. Devi, R. Madivanane, *Eng. Sci. Technol.,* **2012**. *2*, 795.

[22] C. L. E. Nijst, J. P. Bruggeman, J. M. Karp, L. Ferreira, A. Zumbuehl, C. J. Bettinger, R. Langer, *Biomacromolecules* **2007**, *8*, 3067.

[23] K. J. Abrams, M. Dapor, N. Stehling, M. Azzolini, S. J. Kyle, J. S. Schäfer, A. Quade, F. Mika, S. Kratky, Z. Pokorna, I. Konvalina, D. Mehta, K. Black, C. Rodenburg, *Adv. Sci.* **2019**, *6*, 1900719.

[24] R. C. Masters, N. Stehling, K. Abrams, V. Kumar, M. Azzoloni, N. M. Pugno, M. Dapor, A. Huber, P. Schäfer, D. G. Lidzey, C. Rodenburg, *Adv. Sci.* **2019**, *6*, 1801752.

[25] C. C. Yeh, C. N. Chen, Y. T. Li, C. W. Chang, M. Y. Cheng, H. I. Chang, *Cell. Polym.* **2011**, *30*, 261.

[26] A. V. Shyichuk, J. R. White, I. H. Craig, I. D. Syrotynska, *Polym. Degrad. Stab.* **2005**, *88*, 415.